Geometry of the Poincaré plot of *RR* intervals and its asymmetry in healthy adults

2007 Physiol. Meas. 28 287

(http://iopscience.iop.org/0967-3334/28/3/005)

IOP PUBLISHING PHYSIOLOGICAL MEASUREMENT

Physiol. Meas. **28** (2007) 287–300 doi:10.1088/0967-3334/28/3/005

Geometry of the Poincaré plot of *RR* intervals and its asymmetry in healthy adults

J Piskorski[1] **and P Guzik**[2]

[1] Institute of Physics, University of Zielona Gora, Prof. Szafrana 4a, 65-516 Zielona Gora, Poland
[2] Department of Cardiology-Intensive Therapy, University of Medical Sciences in Poznan, Przybyszewskiego 49, 60-355 Poznan, Poland

E-mail: jaropis@zg.home.pl

Received 24 November 2006, accepted for publication 23 January 2007
Published 19 February 2007
Online at stacks.iop.org/PM/28/287

Abstract

The geometry of the Poincaré plot of *RR* intervals is considered and its basic descriptors are defined in terms of the second moment of a distribution of points in a plane. One of the standard descriptors, SD1, is redefined and used to define two new descriptors, $SD1_{UP}$ and $SD1_{DOWN}$, whose squares partition $SD1^2$ (the variance corresponding to short-term heart rate variability) into contributions from decelerations and accelerations of heart rate. It is shown that there is a visible and statistically highly significant asymmetry in the Poincaré plot, with the upper part, corresponding to decelerations of heart rate, larger than the lower part, which corresponds to accelerations. The effect is shown in one hundred 30 min long time series of *RR* intervals derived from the ECG recordings of 100 young (19–32 years old) and healthy adults. After shuffling the data to random order the asymmetry disappears, which shows that this is a genuine physiological phenomenon rather than an artefact of the method.

Keywords: heart rate variability, Poincaré plot, heart rate asymmetry

M This article features online multimedia enhancements

1. Introduction

The Poincaré plot of *RR* intervals is one of the techniques used in heart rate variability (HRV) analysis. It is both a useful visual tool which is capable of summarizing an entire *RR* time series derived from an electrocardiogram in one picture, and a quantitative technique which gives information on the long- and short-term HRV.

A Poincaré plot of *RR* intervals is composed of points (RR_i, RR_{i+1}), that is each point in the plot corresponds to two consecutive *RR* intervals. The resulting cloud of points is

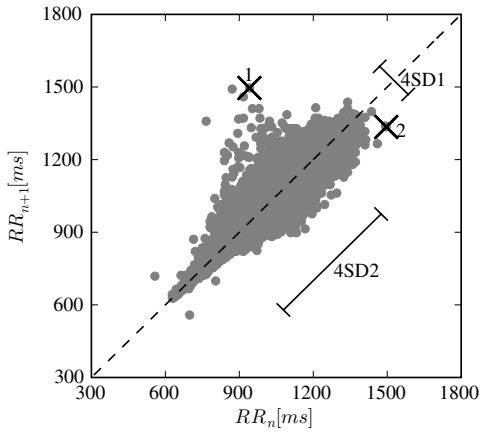

Figure 1. An example Poincaré plot of *RR* intervals of sinus origin only, derived from a 4 h long recording taken from a 25 year old male during sleep, with the basic descriptors. The points marked with a cross correspond to an outlying (but still of sinus origin) point (1) and the consecutive point (2)—for details see section 3 and the discussion. This recording has not been used in the study of section 7, but it has been used as asymmetry (see section 6) is more clearly visible in longer recordings.

usually characterized by its length (SD2) along the line of identity and its breadth across this line (SD1). For reasons given by Brennan *et al* (2001), SD1 is considered to describe the short-term heart rate variability and SD2 the long-term HRV. The precise definitions of SD1 and SD2 are given in section 2.

An example of a Poincaré plot together with its two basic parameters is presented in figure 1.

The visual inspection of the shapes of the Poincaré plot of *RR* intervals is a widely used method for analysing the quality of recorded ECG signals and identification of premature and ectopic beats, as well as technical artefacts (Mourot *et al* 2004a, Sosnowski *et al* 2005). This method also describes the effects of sympathetic and parasympathetic influences on heart rate (Kamen *et al* 1996, Brennan *et al* 2002, Toichi *et al* 1997). As such, it has been applied in various physiological studies evaluating the influence of catecholamines or autonomic blockage on HRV, changes of autonomic modulation of heart rate during sleep, exercise or paced breathing (Mourot *et al* 2004a, Kamen *et al* 1996, Brennan *et al* 2002, Toichi *et al* 1997, Otzenberger *et al* 1998, Mourot *et al* 2004b, Tulppo *et al* 1996, 1998, Guzik *et al* 2005b). The Poincaré plot method also provides prognostic information about mortality in post-myocardial infarction, chronic heart failure, and sudden infant death syndrome and about the risk of life threatening ventricular arrhythmias in patients subjected to cardiac surgery (Woo *et al* 1992, Schechtman *et al* 1992, Makikallio *et al* 1997, Huikuri *et al* 1996, Hnatkova *et al* 1995, Stein *et al* 2005). It has also been used in other clinical settings like stroke, diabetes, chronic renal failure, in patients after coronary artery bypass grafting or with sleep apnea syndrome (Korpelainen *et al* 1999, Guzik *et al* 2005a, Laitio *et al* 2002, Aljadeff *et al* 1997).

The present paper has two aims. The first of them is to analyse the geometry of the Poincaré plot in detail and to define its basic parameters using geometric language. This approach, compared to the usual time-domain statistical approach, offers a different perspective on the interpretation of Poincaré plot descriptors. The second is an attempt to describe a visible feature of the Poincaré plot, namely that a typical plot is usually clearly asymmetric. We develop the necessary tools for studying this phenomenon by defining new Poincaré plot

descriptors which quantify the asymmetry and describing statistical procedures for handling them. We also go further and claim that the Poincaré plot asymmetry is one-way, that is that the upper part of the Poincaré plot is 'bigger' than the lower.

To support the theoretical discussion we present the result of a study on a hundred 30 min long *RR* time series which shows that there is a clear one-way asymmetry in the sample. This one-way asymmetry is called here *heart rate asymmetry* (HRA), and on the basis of the studies presented in this paper and in Guzik *et al* (2006), we suggest that it may be a feature characteristic of recordings from resting subjects.

The paper is organized as follows: in section 2 we describe the standard Poincaré plot descriptors; however, we do so with the use of geometric language rather than the usual statistical language. Section 3 discusses the special status of the line of identity of a Poincaré plot. In section 4 the standard short-term HRV descriptor SD1 is redefined to reflect the second moment of the Poincaré plot points distribution around the line of identity, rather than the line parallel to the line of identity, passing through the centroid. We show that in spite of the changed definition the redefined SD1 is numerically almost indistinguishable from the traditional SD1, but it is easier to understand. Section 5 presents the main theoretical result of the present paper, namely the two new asymmetric descriptors $SD1_{UP}$ and $SD1_{DOWN}$. These parameters are derived (with the use of the theory developed in sections 2, 3 and 4) and discussed. In section 6 we define what is meant by heart rate asymmetry and describe the statistical tools which can be used to check for its presence. Section 7 contains a study involving a hundred 30 min long ECGs where we put to use the theory developed in sections 2–6 and show that HRA is clearly present in the studied group. To check the validity of the method we repeat all the calculations for the same data after random shuffling. In this case the asymmetry vanishes, which indicates that HRA is a genuine physiological phenomenon, rather than an artefact of the method.

In the last section we discuss the phenomenon from both the physiological and mathematical points of view.

Appendix A contains a short proof that the geometric Poincaré plot descriptors derived in section 2 are equivalent to the descriptors commonly used in HRV research. In appendix B we show how to code the new and old Poincaré plot descriptors in Matlab, Octave and other matrix programming languages. Appendix C describes the animation that illustrates the behaviour of the centroid and other parameters associated with a Poincaré plot in time.

2. Standard Poincaré plot descriptors

A typical Poincaré plot is shown in figure 1. For a healthy person, it is usually a cloud of points in the shape of an ellipse or a comet (Brennan *et al* 2001, 2002). The two basic parameters describing this cloud are SD1 and SD2—they are customarily called the Poincaré plot *descriptors*. Both descriptors are shown in figure 1. The formulae for these descriptors may be found in Brennan *et al* (2001) or in appendix A of the present paper. As will be seen, $SD1^2$ is the second moment of the distribution of the cloud around l_1 (compare figure 2) and $SD2^2$ is the second moment of this distribution around l_2. The slope of l_1 is $\pi/4$ and the slope of l_2 is $3\pi/4$. Both these lines pass through the centroid of the cloud (compare figure 2.)

In Brennan *et al* (2001) and Piskorski and Guzik (2005) the definitions of SD1 and SD2 are given in terms of variance of transformed and projected (RR_i, RR_{i+1}) pairs. Here, we will use the geometric language of the second moment with respect to a straight line and give an equivalent definition using this language. This approach will prove useful in latter parts of the paper.

Let **RR**, **x** and **y** vectors be defined as

$$\begin{aligned}\mathbf{RR} &\equiv (RR_1, RR_2, \ldots, RR_n, RR_{n+1}),\\ \mathbf{x} &\equiv (x_1, x_2, \ldots, x_n) \equiv (RR_1, RR_2, \ldots, RR_n)\\ \mathbf{y} &\equiv (y_1, y_2, \ldots, y_n) \equiv (RR_2, RR_3, \ldots, RR_{n+1}),\end{aligned} \tag{1}$$

where RR_i stands for the ith RR interval, and n is the number of points in the Poincaré plot (which is one less than the length of the **RR** time series). Using the above, the Poincaré plot of RR intervals can be defined as the ordered pairs (points in a plane) (x_i, y_i) (Piskorski and Guzik 2005). The centroid, or the first moment (x_C, y_C) of a distribution of n points (x, y) is defined in the following way:

$$\sum_{i=1}^{n} x_C = \sum_{i=1}^{n} x_i, \qquad \sum_{i=1}^{n} y_C = \sum_{i=1}^{n} y_i, \tag{2}$$

which in our case yields the centroid of the Poincaré plot as

$$x_C = \bar{x}_i, \qquad y_C = \bar{y}_i. \tag{3}$$

The overbar stands for *mean*.

The lines l_1 and l_2 described above can be defined as

$$l_1 : y - y_C = \tan\left(\frac{\pi}{4}\right)(x - x_C), \qquad l_2 : y - y_C = \tan\left(\frac{3\pi}{4}\right)(x - x_C).$$

After some algebra, we express the distance of the ith Poincaré plot point from l_1 and l_2, respectively, as

$$d_i^1 = \frac{|(x_i - x_C) - (y_i - y_C)|}{\sqrt{2}}, \qquad d_i^2 = \frac{|(x_i - x_C) + (y_i - y_C)|}{\sqrt{2}}. \tag{4}$$

Consequently, we obtain the following formulae for $\mathrm{SD1}_C$ and $\mathrm{SD2}_C$:

$$\mathrm{SD1}_C^2 = \frac{1}{n}\sum_{i=1}^{n}\left(d_i^1\right)^2, \tag{5}$$

$$\mathrm{SD2}_C^2 = \frac{1}{n}\sum_{i=1}^{n}\left(d_i^2\right)^2. \tag{6}$$

In appendix A we show that these formulae are exactly equivalent to the definitions of SD1 and SD2 given in Brennan *et al* (2001).

The derivation presented in this section is illustrated by figure 2.

3. The line of identity of the Poincaré plot

The identity line $(y = x)$ in the Poincaré plot has a simple physiological interpretation: the points on this line correspond to equal consecutive RR intervals, the points above it correspond to decreasing heart rate and the points below this line to increasing heart rate.

A period of increasing heart rate must be followed by a decrease and vice versa. The same can be said of isolated events, when an RR interval is significantly longer or shorter than the preceding interval. In such a case it is very probable that the next interval will be shorter or longer, respectively, which will flip the outlying point connected with such an event from one side of the identity line to the other, although this flip will not usually be a mirror reflection

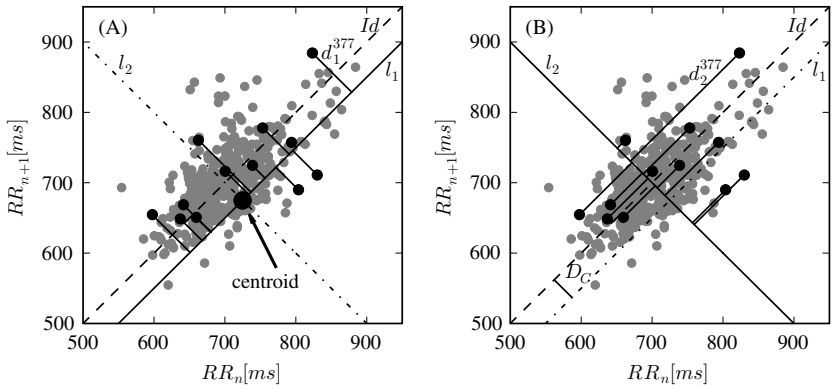

Figure 2. Calculation of the standard Poincaré plot descriptors with the use of geometric language. The value of D_C, which is the perpendicular distance from the identity line to the centroid (or l_1), is exaggerated by a few orders of magnitude for better readability. Id stands for *Identity line*. For details see text.

(compare figure 1). This is the reason for the apparent symmetry with respect to the line of identity detected by the human eye in the Poincaré plot.

A closer inspection reveals that this symmetry of the Poincaré plot is usually broken, but it is still convenient to define the asymmetry relative to the identity line, i.e. assume that we expect the Poincaré plot to be symmetric with respect to the line of identity and study the departures from this assumed symmetry.

There is another reason for this approach: if there is a line of (approximate) symmetry, then the centroid should lie on this line or in its close vicinity. This is true of the line of identity. The animation shows an example of decomposition of a long recording (4 h) of a healthy person into instantaneous 5 min Poincaré plots. In other words, each frame of the animation shows the Poincaré plot of a 5 min recording, and the frame is updated after each heartbeat (Guzik and Piskorski, 2005). In the animation we can see the dynamic Poincaré plot, the line of identity, l_1 and l_2 and the centroid. As expected, the centroid, and consequently also l_1, stays very close to the identity line for the entire duration of the recording (compare also appendix C).

We see that the line of identity has a special status in the current problem: (1) it has a simple physiological interpretation and (2) it is the best candidate for the single symmetry axis for every Poincaré plot. If the Poincaré plot is asymmetric, it is still useful in studying the departures from symmetry. l_1, which is the basis for calculating the traditional SD1 descriptor, does not have either of these advantages.

4. Second moment of the Poincaré plot with respect to the line of identity

In this section we make use of the properties of the line of identity described above to redefine SD1 so as to give it a clearer physiological interpretation and to allow us to decompose $SD1^2$ into two parts contributed respectively by the points above the identity line (corresponding to the prolongations of *RR* intervals) and the points below it (corresponding to the shortenings of *RR* intervals).

As we saw in section 2, $SD1^2$ is the second moment of the distribution of points forming the Poincaré plot with respect to l_1. As we said in section 3, the identity line has a special

status in the Poincaré plot of *RR* intervals, so let us define the second moment around this line as

$$\mathrm{SD1}_I^2 \equiv \frac{1}{n}\sum_{i=1}^{n} D_i^2, \tag{7}$$

where D_i is the perpendicular distance of each of the Poincaré plot points to the line of identity (see figure 3). D_i can easily be expressed as the length of the cross product:

$$D_i = \left| \begin{pmatrix} x_i \\ y_i \end{pmatrix} \times \frac{\sqrt{2}}{2} \begin{pmatrix} 1 \\ 1 \end{pmatrix} \right| = \frac{|x_i - y_i|}{\sqrt{2}}. \tag{8}$$

From geometry or mechanics it is known that the line through the centroid (l_1) minimizes the second moment in the considered direction, so we have

$$\mathrm{SD1}_I^2 \geqslant \mathrm{SD1}_C^2.$$

Using Steiner's theorem we can write the exact expression for $\mathrm{SD1}_I$ in terms of $\mathrm{SD1}_C$

$$\mathrm{SD1}_I^2 = D_C^2 + \mathrm{SD1}_C^2, \tag{9}$$

D_C is the distance from the centroid to the line of identity. D_C can be easily calculated using formulae (8), (2) and the definitions of vectors **x** and **y**:

$$D_C = \frac{|x_C - y_C|}{\sqrt{2}} = \frac{1}{n}\frac{|x_1 - y_n|}{\sqrt{2}} = \frac{1}{n}\frac{|RR_1 - RR_{n+1}|}{\sqrt{2}},$$

where n is the number of points in the plot. Let us now calculate the difference between $\mathrm{SD1}_I^2$ and $\mathrm{SD1}_C^2$:

$$\Delta \equiv \mathrm{SD1}_I^2 - \mathrm{SD1}_C^2 = \frac{1}{n^2}\frac{(RR_1 - RR_{n+1})^2}{2}, \tag{10}$$

so finally we get

$$\lim_{n\to\infty} \Delta = 0. \tag{11}$$

The two second moments $\mathrm{SD1}_I^2$ and $\mathrm{SD1}_C^2$ are then approximately equal in the case of the Poincaré plot of *RR* intervals. In the study presented in section 7 the mean difference $\overline{\Delta} = 2.3 \times 10^{-5}\,\mathrm{s}^2$, and the average relative error introduced by the changed definition is 3.1×10^{-8}, so small that it is of no practical importance.

Thus, $\mathrm{SD1}_I^2$ and $\mathrm{SD1}_C^2$ are numerically very close, but their mathematical properties are different. $\mathrm{SD1}_C^2$ minimizes the second moment (so it is equivalent to variance) in the direction of the line of identity, and $\mathrm{SD1}_I^2$ measures the second moment around the physiologically meaningful line of identity. Since the second moment minimizing property does not seem to have any practical value in the analysis of the Poincaré plot of *RR* intervals, and since the numerical difference between the two is so small, we suggest that the definition (7) of $\mathrm{SD1}_I^2$ be used as the basis for defining SD1. In fact, the discussion showing that SD1 is a measure of short-time variability presented in Brennan *et al* (2001) uses the line of identity rather than l_1 and the centroid.

From our point of view, the most important property of $\mathrm{SD1}_I^2$ is the fact that it is possible to partition this second moment into two parts—the contribution from the points above the line of identity (decelerations of heart rate) and the contribution from the points below the line of identity (accelerations).

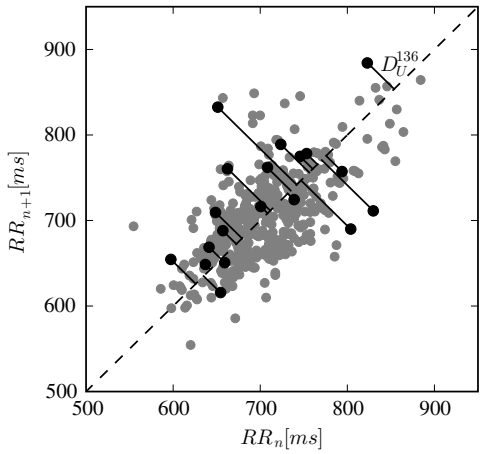

Figure 3. Calculation of the redefined SD1 descriptor. D_U^{136} is the distance from the point number 136, which is one of the points located above the identity line, to the identity line. See sections 5 and 6 for details.

5. Measures of asymmetry of the Poincaré plot

If we distinguish the points above the line of identity from the points below it, we can rewrite equation (7) as

$$\mathrm{SD1}_I^2 = \frac{1}{n}\left(\sum_{i=1}^{n_U}\left(D_U^i\right)^2 + \sum_{i=1}^{n_D}\left(D_D^i\right)^2 + \sum_{i=1}^{n_O}\left(D_O^i\right)^2\right) \tag{12}$$

$$= \frac{1}{n}\left(\sum_{i=1}^{n_U}\left(D_U^i\right)^2 + \sum_{i=1}^{n_D}\left(D_D^i\right)^2\right), \tag{13}$$

where D_U^i is the distance of the ith point above the line of identity (compare figure 3) and D_D^i and D_O^i mean the same for the points below and on the line of identity (U, D and O stand for *Up*, *Down* and *On*, respectively). Similarly, n_U is the number of points above the line of identity, and n_D and n_O mean the same for the points below and on the line of identity. Additionally,

$$D_O^i \equiv 0 \qquad \text{for all} \quad i \qquad \text{and} \qquad n_U + n_D + n_O = n. \tag{14}$$

We are now in a position to define the contributions from the points above and below the identity line to $\mathrm{SD1}^2$:

$$\mathrm{SD1}_I^2 = \mathrm{SD1}_{\mathrm{UP}}^2 + \mathrm{SD1}_{\mathrm{DOWN}}^2, \tag{15}$$

where

$$\mathrm{SD1}_{\mathrm{UP}}^2 \equiv \frac{1}{n}\sum_{i=1}^{n_U}\left(D_U^i\right)^2, \qquad \mathrm{SD1}_{\mathrm{DOWN}}^2 \equiv \frac{1}{n}\sum_{i=1}^{n_D}\left(D_D^i\right)^2. \tag{16}$$

In this way we have partitioned the second moment around the identity line into two parts corresponding separately to accelerations ($\mathrm{SD1}_{\mathrm{UP}}$) and decelerations ($\mathrm{SD1}_{\mathrm{DOWN}}$) of the heart rate. It should be noted that $\mathrm{SD1}_{\mathrm{UP}}$ and $\mathrm{SD1}_{\mathrm{DOWN}}$ are not standard deviations.

Heart rate variability is very different in various subjects, so some kind of normalization of the above parameters might be helpful. Let us define the following relative contributions to

$\mathrm{SD1}_I^2$ from accelerations and decelerations of heart rate:

$$\begin{aligned} C_{\mathrm{UP}} &\equiv \frac{\mathrm{SD1}_{\mathrm{UP}}^2}{\mathrm{SD1}_I^2}, && \text{for decelerations} \\ C_{\mathrm{DOWN}} &\equiv \frac{\mathrm{SD1}_{\mathrm{DOWN}}^2}{\mathrm{SD1}_I^2}, && \text{for accelerations.} \end{aligned} \tag{17}$$

These parameters (possibly multiplied by 100%) can be compared between subjects and used for exploratory data analysis, i.e. barplots, histograms etc.

The above derivations would be just a mathematical exercise, were it not for the fact that Poincaré plots of *RR* intervals exhibit a highly significant one-directional asymmetry, at least in resting recordings from healthy subjects.

6. Heart rate asymmetry in Poincaré plots of *RR* intervals

In this section we define the heart rate asymmetry which is visible in Poincaré plots of *RR* intervals and describe the statistical tools for analysing it.

Visually, HRA means that the top part of the Poincaré plot (above the line of identity) usually seems 'bigger' than the part below the identity line (see for example figure 1—asymmetry is also visible in figures 2 and 3). The discussion presented so far allows us to give the adjective 'bigger' a precise mathematical meaning, as $\mathrm{SD1}_{\mathrm{UP}}$ and $\mathrm{SD1}_{\mathrm{DOWN}}$ quantify the sizes of the respective parts and make it possible to compare them and draw statistical conclusions.

If the magnitudes of $\mathrm{SD1}_{\mathrm{UP}}$ and $\mathrm{SD1}_{\mathrm{DOWN}}$ were subject to random fluctuations only, we would observe in a group of N recordings that approximately half of them have $\mathrm{SD1}_{\mathrm{UP}} > \mathrm{SD1}_{\mathrm{DOWN}}$ and half $\mathrm{SD1}_{\mathrm{UP}} \leqslant \mathrm{SD1}_{\mathrm{DOWN}}$.

To study the statistical significance of the effect we suggest using the binomial test. Let us assume that we have N recordings for which we have calculated $\mathrm{SD1}_{\mathrm{UP}}$ and $\mathrm{SD1}_{\mathrm{DOWN}}$ and established that N_1 of them have $\mathrm{SD1}_{\mathrm{UP}} > \mathrm{SD1}_{\mathrm{DOWN}}$ and $N_2 = N - N_1$ have $\mathrm{SD1}_{\mathrm{UP}} \leqslant \mathrm{SD1}_{\mathrm{DOWN}}$. If P is the population proportion of recordings with $\mathrm{SD1}_{\mathrm{UP}} > \mathrm{SD1}_{\mathrm{DOWN}}$ then we can use the sample proportion $\bar{P} = N_1/N$ as an estimate of P and test the hypothesis $H_0 : P = 1/2$ against the alternative hypothesis $H_1 : P > 1/2$ using a one-sided binomial test. We can use the results reported in Guzik *et al* (2006) to calculate the necessary sample size. Let us choose the significance level $\alpha = 0.05$ and the power of the test $1 - \beta = 0.8$. The sample proportion obtained in Guzik *et al* (2006) is $\bar{P} = 0.82$ so for the purpose of calculating the sample size we choose $P_s = 0.7$, which is a conservative choice. The sample size calculation for the one-sided binomial test with the above assumptions yields the sample size $N_0 = 74$.

The relative contributions C_{UP} and C_{DOWN} can also be used for significance testing in conjunction with the distribution free matched pairs Wilcoxon test. This test, being a non-parametric, combinatorial test, will not be more powerful than the binomial test, but it may be more appealing to researchers with a medical background. It should also be noted that this test requires symmetry around the median, which may not always be fulfilled.

7. The study

In this section we calculate the parameters defined above and verify the heart rate asymmetry hypothesis in a group of 100 recordings of length 30 min. We also verify the method by shuffling each recording so as to obtain an **RR** vector in random, rather than physiological,

order. If the asymmetry is an artefact of the method it should also be present in the shuffled data. If, on the other hand, asymmetry vanishes after shuffling, we can assume that it is a genuine physiological phenomenon.

7.1. Materials and methods

7.1.1. Subjects. One hundred healthy volunteers (19–32 years old; 47 female) were enrolled. All subjects refrained from smoking, alcohol and coffee for 24 h prior to the study. No participant was addicted to drugs, taking any medications, or involved in endurance training. Forty three participants were occasional smokers, while the rest were nonsmokers. All volunteers gave informed consent to participate in the study. This project was approved by the University Bioethics Committee.

7.1.2. Protocol. The study was performed at rest in the supine position, and the subjects were kept quiet in a neutral environment. The subjects were allowed to breathe spontaneously during the whole study. The 30 min recording was taken after a preceding 15 min period used for cardiovascular adaptation. Three channels of a bipolar chest lead ECG were recorded with a sampling frequency of 1600 Hz by an A/D converter (Porti 5, TMSI, The Netherlands). The data were transferred on-line to a PC for on-screen monitoring and data storage. The preliminary automatic evaluation of the recordings was performed with the use of the libRASCH/RASCHlab software from the libRASCH project (v. 0.6.1; http://www.librasch.org, Germany). This was then followed by visual inspection of all signals and necessary corrections of the obtained values (Schneider *et al* 2004). The values of the RR intervals were retrieved from the stored recordings and used in further analysis.

The data were analysed with the use of in-house software written in Python (Python Foundation, USA) and Matlab (MathWorks, USA). The statistical analysis was performed with the use of the R statistical package (R-project, www.r-project.org).

7.2. Results

In the 100 recordings we observed $SD1_{UP} > SD1_{DOWN}$ in 81 cases, which yields the p-value in the binomial test $p < 10^{-10}$. The estimated probability is, obviously, $\bar{P} = 0.81$ and the 95% confidence interval $(0.72, 0.89)$. We can conclude that the hypothesis of equal probability of getting $SD1_{UP} > SD1_{DOWN}$ and $SD1_{UP} \leqslant SD1_{DOWN}$ must be rejected and it is far more likely that in a Poincaré plot the upper part will be 'bigger' than the part below the line of identity.

The Wilcoxon test (paired, one sided, signed rank test with continuity correction) yields the p-value $p < 10^{-9}$. The estimated difference of the sample medians is $\Delta\mu = \mu(C_{UP}) - \mu(C_{DOWN}) = 0.5436 - 0.4566 = 0.087$ and the nonparametric 95% confidence interval $(0.06, 0.11)$, which rejects the hypothesis that the median of C_{UP} is equal to the median of C_{DOWN}.

As can be seen, both tests agree and the results of both tests are highly significant.

7.3. Results for shuffled data

After shuffling the same data to random order we obtained 52 cases in which $SD1_{UP} > SD1_{DOWN}$, so the p-value in the binomial test for the hypothesis that it is equally probable to get the lower and the upper part of the Poincaré plot bigger is $p = 0.76$, the estimated $\bar{P} = 0.52$ and the 95% confidence interval is $(0.42, 0.62)$, so the postulated $P = 0.5$ is well

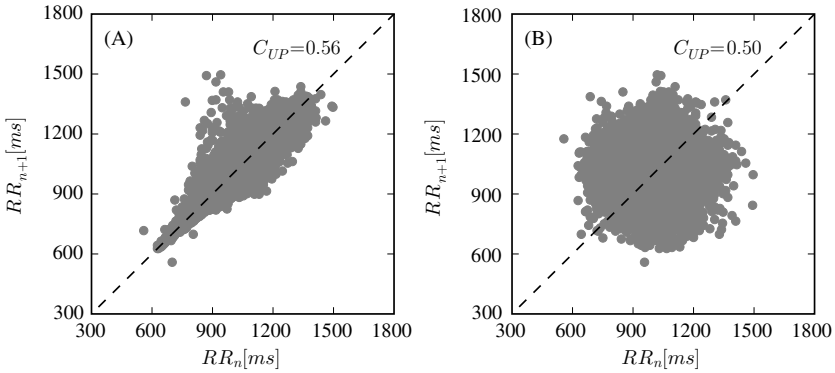

Figure 4. The Poincaré plot for the same recording as in figure 1 in the physiological order (panel A) and after shuffling (panel B). After shuffling, the Poincaré plot loses both its autocorrelation structure (i.e., becomes circular) and asymmetry.

within this interval. This means that the differences between $SD1_{UP}$ and $SD1_{DOWN}$ should be attributed to random fluctuation only.

In the Wilcoxon test for equality of the medians of C_{UP} and C_{DOWN} we get $p = 0.40$ with the estimated difference of the medians $\Delta\mu = 0.0014$ and the nonparametric 95% confidence interval is $(-0.0019, 0.0045)$, so the value 0 corresponding to both medians equal lies within this interval. This result indicates that the contributions to the variance from the upper part of the Poincaré plot (C_{UP}) are the same as the contributions from the lower parts (C_{DOWN}).

The results of shuffling the data may be seen in figure 4. It is clear that after shuffling the asymmetry disappears.

Once again both tests agree and give unambiguous results.

8. Discussion

In the present paper we have considered the geometry of the Poincaré plot from the point of view of the second moment of the distribution of points in a plane. We have defined the standard Poincaré plot descriptors using geometric language and redefined one of them, namely SD1. It has been shown that the redefinition does not significantly change the numerical value of SD1. The redefined descriptor has a useful property of being calculated with respect to the same line, the line of identity, for each Poincaré plot rather than the line passing through the centroid of the cloud. This property allowed us to define two new descriptors, $SD1_{UP}$ and $SD1_{DOWN}$, which measure the respective contributions of the points above the identity line (decelerations) and below it (accelerations) to the short-term heart rate variability described by SD1.

We applied the above to a study involving a hundred 30 min long recordings. We have shown that there is a one-directional asymmetry in the Poincaré plot of *RR* intervals, with the part above the line of identity larger than the part below it. We call this observation *heart rate asymmetry*. With the use of the binomial test and, independently, the matched pairs Wilcoxon test, we have shown that this phenomenon is statistically highly significant. To check if the phenomenon is a genuine physiological phenomenon we have used the shuffled data approach in which all *RR* recordings were shuffled to random order. In this case there was no asymmetry.

The interpretation of these findings seems to be very difficult. This asymmetry cannot be fully explained by the fact that accelerations of heart rate are suppressed more strongly than

decelerations and/or that decelerations are favoured. The construction of the Poincaré plot is such that a sudden deceleration or acceleration is reflected on both sides of the line of identity and, if there were no additional mechanism, would influence $SD1_{UP}$ and $SD1_{DOWN}$ equally (compare the introduction). The nature of this mechanism may be gleaned from figure 1—the outlying point above the line of identity is flipped to the other side, but after the flip it is much closer to this line. This contributes much more to $SD1_{UP}$ than to $SD1_{DOWN}$.

From the mathematical point of view it can be said that the asymmetry is the result of different patterns of accelerations and decelerations of heart rate. In other words, the behaviour of the heart rate after a (sudden) deceleration is qualitatively different from the behaviour after a (sudden) acceleration. However, we do not know what may be the cause of this difference or even what these patterns are.

What we have learnt so far is that HRA is a clearly visible and quantifiable phenomenon in resting healthy people. Previously (Guzik *et al* 2006), we were able to see HRA in 41 out of 50 recordings of 5 min duration. In the current study with the 30 min recordings, HRA is present in a similar proportion of subjects, i.e. about 80%, so it seems that HRA is not affected by the duration of ECG recording. We have not yet established whether HRA is a characteristic of an individual, i.e. independent of time, or if it changes in time (i.e., due to the circadian rhythm or different activities). We do not know why HRA is missing in some subjects, either.

An approach to HRV that may be useful in explaining and perhaps using the asymmetry is phase rectified signal averaging (PRSA)—see Bauer *et al* (2005). In this method the patterns of acceleration and deceleration are analysed and parameters called deceleration/acceleration capacity (DC/AC) are defined. One of these parameters (DC) proves to have a very strong predictive value (Bauer *et al* 2006).

The practical use of the results presented in this paper has yet to be found, but they are interesting from the theoretical point of view. It seems that the analysis of the acceleration/deceleration patterns may contribute to our knowledge and a better understanding of HRV physiology, and perhaps provide us with diagnostically useful parameters.

Appendix A

In this appendix the equivalence of equation (8) in Brennan *et al* (2001) with formula (5) will be shown.

Let us start with the above formula in Brennan *et al* (2001):

$$\mathrm{SD1}^2 = \mathrm{Var}\left(\frac{1}{\sqrt{2}}\mathbf{RR_n} - \frac{1}{\sqrt{2}}\mathbf{RR_{n+1}}\right).$$

The definition of vectors $\mathbf{RR_n}$, $\mathbf{RR_{n+1}}$ is equivalent to definition (1) of $\mathbf{x}$, $\mathbf{y}$, so using (2) and (4) we may write

$$\begin{aligned}\mathrm{SD1}^2 &= \mathrm{Var}\left(\frac{1}{\sqrt{2}}\mathbf{x} - \frac{1}{\sqrt{2}}\mathbf{y}\right)\\ &= \frac{1}{n}\sum_{i=1}^{n}\frac{(x_i - \bar{x} - y_i + \bar{y})^2}{2}\\ &= \frac{1}{n}\sum_{i=1}^{n}\frac{((x_i - x_C) - (y_i - y_C))^2}{2}\\ &= \frac{1}{n}\sum_{i=1}^{n}\left(d_i^1\right)^2. \qquad \text{QED}\end{aligned}$$

Appendix B. The Matlab implementation

For the reader's convenience, this appendix contains the implementation of the descriptors presented in this paper in the Matlab programming language.

Let us assume that the vector variable RR contains the time series of *RR* intervals. The **x** and **y** vectors (1) are defined in the following way:

```
x = RR;    x(end) = [];
y = RR;    y(1) = [];
L = length(x);
```

If the *RR* time series contains ectopic beats it can be filtered with the use of methods presented in Piskorski and Guzik (2005).

The standard descriptors are defined by (5) or in appendix A:

```
SD1C = sqrt((1/L) * sum(((x - y) - mean(x - y)).^2)/2);
SD2C = sqrt((1/L) * sum(((x + y) - mean(x + y)).^2)/2);
```

In this case we could have used the `std` function for calculating the standard deviation, but this function returns the sample standard deviation, that is a value corrected by the $n/(n-1)$ factor. While there is little numerical difference between `std` and the above, we choose to be exact in this paper.

The redefined descriptor $SD1_I$ defined by (7), which is numerically almost identical to $SD1_C$ above:

```
SD1I = sqrt((1/L) * (sum((x - y).^2)/2));
```

The asymmetric descriptors defined by (16) are slightly more difficult to calculate, as we have to find the points above and below the line of identity first. The code is the following:

```
xy = (x - y)/sqrt(2);
indices_up = find(xy > 0);
indices_down = find(xy < 0);
SD1UP = sqrt(sum(xy(indices_up).^2)/L);
SD1DOWN = sqrt(sum(xy(indices_down).^2)/L);
```

Finally, the relative contributions (17):

```
CUP = SD1UP^2/SD1I^2;
CDOWN = SD1DOWN^2/SD1I^2;
```

Appendix C. The animation

The animation is available as an AVI file from the online version of this journal, see stacks.iop.org/PM/28/287. It presents an example of decomposition of a 4 h long recording from a healthy, 25 year old male during sleep . The decomposition technique divides the entire recording into instantaneous 5 min long segments for which a Poincaré plot is produced. The window is moved after each heartbeat and the frame is updated (Guzik and Piskorski 2005).

Panel A (compare figure 5) shows the full decomposition and panel B is a close-up. The centroid of the Poincaré plot is located at the point where l_1 and l_2 cross. The movement of the line parallel to the line of identity (l_1) is almost invisible in panel A—it takes a close-up to see that it changes with each new instantaneous Poincaré plot. This demonstrates the fact (proved

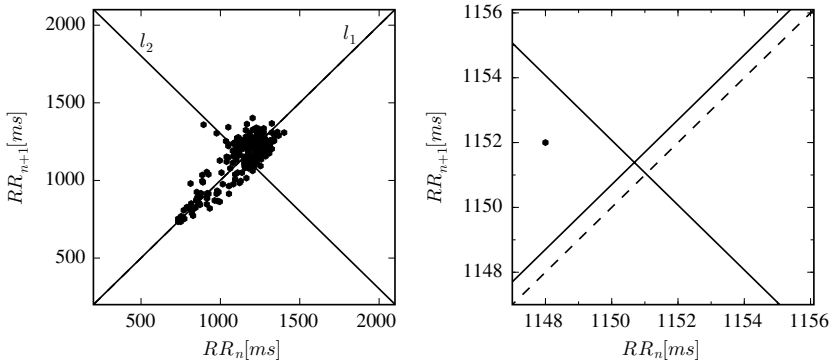

Figure 5. A frame from the animation—type: avi file, size: 2.8 Mb.

in section 4) that the difference between $SD1_C$ and $SD1_I$ is very small. The movement of the line perpendicular to the line of identity (l_2) is clearly visible in both panels, although in panel B it is visible only for very short periods of time, as it spends more time in the areas not covered by the close-up.

References

Aljadeff G, Gozal D, Schechtman V L, Burrell B, Harper R M and Ward S L 1997 Heart rate variability in children with obstructive sleep apnea *Sleep* **20** 151–7

Bauer A, Kantelhardt J W, Bunde A, Barthel P, Schneider R, Malik M and Schmidt G 2005 Phase-rectified signal averaging detects quasi-periodicities in non-stationary data *Physica* A **364** 423–34

Bauer A *et al* 2006 Deceleration capacity of heart rate as a predictor of mortality after myocardial infarction: cohort study *Lancet* **367** 1674–81

Brennan M, Palaniswami M and Kamen P 2001 Do existing measures of Poincaré plot geometry reflect nonlinear features of heart rate variability? *IEEE Trans. Biomed. Eng.* **48** 1342–47

Brennan M, Palaniswami M and Kamen P 2002 Poincaré plot interpretation using a physiological model of HRV based on a network of oscillators *Am. J. Physiol. Heart Circ. Physiol.* **283** H1873–86

Guzik P, Bychowiec B, Piskorski J, Wegrzynowski A, Krauze T, Schneider R, Liszkowski P, Wykretowicz A, Wierusz-Wysocka B and Wysocki H 2005a Heart rate variability by Poincaré plot and spectral analysis in young healthy subjects and patients with type 1 diabetes *Folia Cardiol.* **12** (suppl. D) 64–7

Guzik P and Piskorski J 2005 Decomposition of the comet-like Poincaré plots of RR intervals *Folia Cardiol.* **12** (suppl. D) O271–4

Guzik P, Piskorski J, Krauze T, Schneider R, Wesseling K H, Wykretowicz A and Wysocki H 2005b The influence of changing respiratory rate on HRV is portrayed by descriptors of Poincaré plot analysis *Folia Cardiol.* **12** (suppl. D) 17–20

Guzik P, Piskorski J, Krauze T, Wykretowicz A and Wysocki H 2006 Heart rate asymmetry by Poincaré plots *Biomed. Tech.* **51** 272–5

Hnatkova K, Copie X, Staunton A and Malik M 1995 Numeric processing of Lorenz plots of R-R intervals from long-term ECGs. Comparison with time-domain measures of heart rate variability for risk stratification after myocardial infarction *J. Electrocardiol.* **28** (Suppl.) 74–80

Huikuri H V, Seppanen T, Koistinen M J, Airaksinen J, Ikaheimo M J, Castellanos A and Myerburg R J 1996 Abnormalities in beat-to-beat dynamics of heart rate before the spontaneous onset of life-threatening ventricular tachyarrhythmias in patients with prior myocardial infarction *Circulation* **93** 1836–44

Kamen P W, Krum H and Tonkin A M 1996 Poincare plot of heart rate variability allows quantitative display of parasympathetic nervous activity in humans *Clin. Sci. (Lond)* **91** 201–8

Korpelainen J T, Sotaniemi K A, Makikallio A, Huikuri H V and Myllyla V V 1999 Dynamic behavior of heart rate in ischemic stroke *Stroke* **30** 1008–13

Laitio T T *et al* 2002 Relation of heart rate dynamics to the occurrence of myocardial ischemia after coronary artery bypass grafting *Am. J. Cardiol.* **15** 1176–81

Makikallio T H, Seppanen T, Airaksinen K E, Koistinen J, Tulppo M P, Peng C K, Goldberger A L and Huikuri H V 1997 Dynamic analysis of heart rate may predict subsequent ventricular tachycardia after myocardial infarction *Am. J. Cardiol.* **80** 779–83

Mourot L, Bouhaddi M, Perrey S, Cappelle S, Henriet M T, Wolf J P, Rouillon J D and Regnard J 2004a Decrease in heart variability with overtraining: assessment by the Poincaré plot analysis *Clin. Physiol. Funct. Imaging* **24** 10–8

Mourot L, Bouhaddi M, Perrey S, Rouillon J D and Regnard J 2004b Quantitative Poincaré plot analysis of heart rate variability: effect of endurance training *Eur. J. Appl. Physiol.* **91** 79–87

Otzenberger H, Gronfier C, Simon C, Charloux A, Ehrhart J, Piquard F and Brandenberger G 1998 Dynamic heart rate variability: a tool for exploring sympathovagal balance continuously during sleep in men *Am. J. Physiol. Heart Circ. Physiol.* **275** H946–50

Piskorski J and Guzik P 2005 Filtering Poincaré plots *Comput. Methods Sci. Tech.* **11** 39–48

Schechtman V L, Raetz S L, Harper R K, Garfinkel A, Wilson A J, Southall D P and Harper R M 1992 Dynamic analysis of cardiac R-R intervals in normal infants and in infants who subsequently succumbed to the sudden infant death syndrome *Pediatr. Res.* **31** 606–12

Schneider R, Barthel P, Bauer A and Schmidt G 2004 libRASCH—a programming framework for signal handling *Comput. Cardiol.* **31** 53–6

Sosnowski M, Clark E, Latif S, Macfarlane P W and Tendera M 2005 Heart rate variability fraction—a new reportable measure of 24-hour R-R interval variation *Ann. Noninvasive Electrocardiol.* **10** 7–15

Stein P K, Domitrovich P P, Huikuri H V and Kleiger R E (Cast Investigators) 2005 Traditional and nonlinear heart rate variability are each independently associated with mortality after myocardial infarction *J Cardiovasc. Electrophysiol.* **16** 13–20

Toichi M, Sugiura T, Murai T and Sengoku A 1997 A new method of assessing cardiac autonomic function and its comparison with spectral analysis and coefficient of variation of R-R interval *J. Auton. Nerv. Syst.* **62** 79–84

Tulppo M P, Makikallio T H, Seppanen T, Airaksinen J K and Huikuri H V 1998 Heart rate dynamics during accentuated sympathovagal interaction *Am. J. Physiol. Heart Circ. Physiol.* **274** H810–6

Tulppo M P, Makikallio T H, Takala T E, Seppanen T and Huikuri H V 1996 Quantitative beat-to-beat analysis of heart rate dynamics during exercise *Am. J. Physiol.* **271** H244–52

Woo M A, Stevenson W G, Moser D K, Trelease R B and Harper R M 1992 Patterns of beat-to-beat heart rate variability in advanced heart failure *Am. Heart. J. Heart Circ. Physiol.* **123** 704–10